

Calibration of DEM parameters for cohesionless bulk materials under rapid flow conditions and low consolidation

Katterfeld, Andre ; Coetzee, Corne ; Donohue, Timothy ; Fottner, Johannes ; Grima, Andrew ; Ramirez Gomez, Alvaro ; Ilic, Dusan ; Kačianauskas, Rimantas ; Necas, Jan ; Schott, D.L.

Publication date

2019

Document Version

Final published version

Citation (APA)

Katterfeld, A., Coetzee, C., Donohue, T., Fottner, J., Grima, A., Ramirez Gomez, A., Ilic, D., Kačianauskas, R., Necas, J., Schott, D. L., Williams, K., & Zegzulka, J. (2019). *Calibration of DEM parameters for cohesionless bulk materials under rapid flow conditions and low consolidation*.

Important note

To cite this publication, please use the final published version (if applicable). Please check the document version above.

Copyright

Other than for strictly personal use, it is not permitted to download, forward or distribute the text or part of it, without the consent of the author(s) and/or copyright holder(s), unless the work is under an open content license such as Creative Commons.

Takedown policy

Please contact us and provide details if you believe this document breaches copyrights. We will remove access to the work immediately and investigate your claim.

White Paper

Calibration of DEM Parameters for Cohesionless Bulk Materials under Rapid Flow Conditions and Low Consolidation

By

Andre Katterfeld	University of Magdeburg, Germany
Corne Coetzee	University of Stellenbosch, South Africa
Timothy Donohue	TUNRA Bulk Solids, Australia
Johannes Fottner	TU Munich, Germany
Andrew Grima	University of Wollongong, Australia
Alvaro Ramirez Gomez	University of Madrid, Spain
Dusan Ilic	The University of Newcastle, Australia
Rimantas Kačianauskas	Vilnius Gediminas Technical University, Lithuania
Jan Necas	TU Ostrava, Czech Republic
Dingena Schott	TU Delft, Netherlands
Kenneth Williams	The University of Newcastle, Australia
Jiri Zegzulka	TU Ostrava, Czech Republic

Last edited 11/07/2019

Prologue

Why a white paper for DEM calibration? Although DEM simulations are increasingly used in many research and industrial fields, a standard approach for the determination of the right contact model parameters does not currently exist. The white paper is aimed to provide an overview about best practices for DEM simulation in the field of bulk material handling. The style of the paper is focussed on a comprehensive overview, not about a discussion or description of certain details. However, such a detailed description is required for the full understanding of the content. Hence, this white paper contains a number of important references.

The white paper is planned as a ongoing project which can be changed and extended regarding the content and authors. The paper makes no claim to completeness but summarises the knowledge and experience of many experts to give an holistic overview of the topic.

1 What is DEM Simulation?

The Discrete Element Method (DEM) was developed by Cundall and Strack [Cun79] in the 1970s in order to solve problems associated with rock mechanics. Cundall and Hart [Cun92] proposed to use the term discrete element method for algorithms that allowed finite displacements and rotations of discrete bodies including their complete separation. Moreover, these algorithms needed to be able to detect new contacts automatically.

The requirements defined above for DEM were also met by event driven methods. In order to distinguish the soft contacts model of finite duration from the event driven methods, Cundall and Strack [Cun79] used the term distinct element method. However, in literature this differentiation is not always followed and often the term distinct element method is replaced by the term discrete element method. In natural sciences the term time driven Molecular Dynamics (MD) is used where, in the 1960s, a variant of the Molecular Dynamics was applied by Rahman [Rah64] to Lennard-Jones-Particles and it is equivalent to DEM.

The potential of DEM was recognized quickly and for research purposes in a number of areas, such as Physics, Nanotechnology, Chemical Engineering and Materials Handling, from which many DEM-algorithms have been devolved.

For the DEM the discrete elements, e.g. the particles of bulk solids, need to be approximated by geometrically describable objects. Since, generally, the transition from a continuum mechanical model to a particle mechanical model leads to much more realistic results, the usage of simple spheres is sufficient for many cases. More complex shapes can be modelled by merging overlapped spheres to form rigid bodies (commonly known as “multispheres”, “clumps”, “glued particles”) or by special mathematical description of non-round particles such as superquadrics or polyhedrons.

The contact points of the particles are described by adequate contact models, such as elastic force displacement laws, Coulomb friction and viscous damping (Fig. 1). Moreover attractive forces such as Van-der-Waals forces and liquid bridge forces can be considered which allows modelling of cohesive particulate systems.

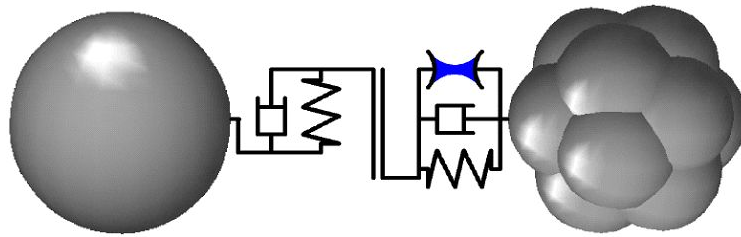


Fig: 1: Example of a contact model for the Discrete Element Method. Spring (elastic force displacement law), dashpot (viscous damping law), frictional element (Coulomb friction), meniscus (pendular liquid bridge) [Grö06]

From all the forces acting on a particle, a resulting force is computed. Using this force the Newtonian equation of motion can be solved for a very short time step, which subsequently delivers the new position and velocity for this particle. This is done for each particle within the system. Therefore, after each time step, new contact detection needs to be performed as new contacts might have formed or existing one might have vanished. By applying this cycle repeatedly the evolution of the particulate system with time is simulated. Machine parts, walls or other boundary conditions can be considered by geometric objects, such as prisms, cylinders, cones and screws.

2 What is Calibration?

Calibration in the DEM context is still understood as a crucial process that should be performed before to claim that a simulation reproduces the behaviour of an assembly of particles in a certain context. It is the inverse process of defining contact model parameters by comparing experimental results with a series of DEM simulations with varying contact model parameters. The set of contact model parameters is chosen which provides a best fit to the experimental result(s).

3 Why Calibrating which DEM Parameters?

Due to the idealisation used in the most DEM simulation models regarding particle size distribution, particle shape and particle stiffness it is necessary to undertake the calibration process to make sure, that the selection of microscopic contact model parameters results in the realistic macroscopic behaviour of the virtual bulk material.

The contact model parameters to be calibrated depend on the used contact model. Often, not all parameters have the same influence on the macroscopic behaviour of the virtual bulk material. The selection of the used contact laws and the influence of the parameter depends on the application scenario. Hence, universal calibration advises are hard to formulate and it seems feasible to develop calibration approaches for a certain application range.

4 Application Oriented Calibration

In the focus of this paper are applications which show a relative fast flow regime of the relatively free flowing cohesionless or low-cohesive bulk materials under low to medium consolidation (< 100 kPa). The consolidation conditions are often generated due to the weight of the bulk material itself or due to an impact. Many scenarios include the establishment of “free surfaces” of the bulk material. Such scenario conditions can be found in many bulk material handling applications including flow, transfer, loading and unloading.

The advice for the following calibration procedure may be less meaningful for other applications such as comminution or compaction processes, impact studies of single bodies or the slow flow of highly consolidated bulk materials in very high silos.

5 Selecting Contact Models for Cohesionless Bulk Material

A large number of contact models are available for use. The contact model laws should be selected according to the application. The most often used contact models for the application scenario of “fast flow regime, low consolidation, free surface flow” includes the Hertz-Mindlin model (no slip) as described in [Rah11] and the simple linear contact model. Other contact models may include hysteresis [Thakur] which permits plastic deformation of the particle assembly once an elastic threshold is attained. Any of these models can be used in conjunction with a modified rolling friction model Typ C according to [Ai12] and [Wen12].

This paper does not declare a standard contact model. However, the definition of a contact model is necessary to determine the number of parameters. Where possible, the parameters are discussed in general terms, in other words, contact model independent. However, in discussing details, reference to specific contact models cannot be avoided.

6 Contact model parameters and influence on bulk material behaviour

All contact models requires the definition of the parameters summarised in the following table. The table further gives some indication and advice about the sensitivity of parameter selection to the simulation and to the macroscopic behaviour of the simulated bulk material under consideration of the above named application scenario (for other scenarios this indication might be wrong). The more contact model parameters which must calibrate, the more effort that is required in the calibration process.

Table 1: Relation between micro-parameters and material bulk behaviour

DEM micro-parameters	Bulk Material Properties (macro-parameters)				DEM model
	<i>Bulk density and porosity including changes due to flow (dilatancy)</i>	<i>Bulk friction / shear / interlocking / flow behaviour</i>	<i>Dissipation of energy (damping)</i>	<i>Bulk stiffness</i>	<i>Computation time</i>
Particle shape	Weak	Strong	Negligible	Negligible	Strong
Particle size distribution	Weak	Weak	Negligible	Negligible	Strong
Contact damping / coefficient of restitution	Negligible	Negligible	Strong	Negligible	Negligible
Contact stiffness	Negligible	Weak	Negligible	Strong	Strong
Particle density	Strong	Negligible	Negligible	Negligible	Strong
Contact sliding friction: particle-particle	Weak	Strong	Strong	Negligible	Negligible
Contact sliding friction: particle-wall	Negligible	Strong	Strong	Negligible	Negligible
Contact rolling friction	Negligible	Strong	Weak	Negligible	Negligible
Experiments that are sensitive to the specific bulk material property	Bulk density/porosity: Filled container Dilatancy: Direct shear test	Angle of repose Discharge test Draw down test Direct shear test	Drop tests Pendulum test Uniaxial compression	Uniaxial compression	-

6.1 Particle Shape

The discrete elements, used in DEM to represent the particles, need to be approximated by geometrically describable objects. Since, generally, the transition from a continuum mechanical model to a particle mechanical model leads to much more realistic results. Single spheres have been commonly used in the earliest models, nowadays complex shapes can be approximated using different techniques; merging overlapping spheres to form rigid bodies (commonly known as “multi-spheres”, “clumps” or “glued particles”) or by special mathematical descriptions of non-spherical particles using superquadric equations, polyhedrons or faceted particles (e.g., created from imported STL models), or through spherical harmonics. These techniques are computationally expensive and some still need to be implemented in DEM codes [Rad16].

Spherical particles are computationally most efficient. However, the contact model for spheres should include rolling resistance to realistically model actual non-spherical particle rotational behaviour. When non-spherical particles are used, rolling resistance can be omitted, even for relatively simple shapes such as a multi-sphere particles comprising only three to four spheres, thereby eliminating the need to calibrate rolling resistance. However, the complexity due to non-spherical shape will make the computational effort less efficient, i.e. increase simulation time. Note that multi-sphere particles with a symmetry axis, for example an ellipsoid, might still need the inclusion of rolling resistance since the particle can easily roll around its axis [Mar10].

It is suggested that spherical particles can be used if the bulk material is relatively homogeneous in terms of particle size and shape. The influence of particle shape also diminishes where the velocity variation of the assembly or flowing stream of particles modelled in the full scale application is not of significance. The larger the particles are in comparison to the modelled range or to the size of the geometric boundaries (e.g. interacting machine parts), the more important is the consideration of the real particle shape. If a non-spherical particle is used, it is proposed to use a simple multi-sphere particle comprising three spheres in a pyramid shape [Coe16]. If mixing rates, internal failure and flow patterns due to mechanical arching, screening or sieving processes should be investigated, the consideration of a more realistic particle shape is of utmost importance [Ch17]. Extreme shaped materials such as biomass will require also an investigation for the best shape approximation. Some approaches are focusing in the seek of algorithms to find an accurate shape without compromising the computational cost [Li15].

The particle shape will influence all the other calibrated parameter values and therefore this should be the first decision made by the modeller. If the shape is changed or adjusted, all the parameter values should be re-calibrated. The effects of particle shape on the individual bulk properties are described below:

1. The particle shape will influence the packing porosity and hence the bulk density for a given particle density. It is difficult to quantify this relation in terms of shape identifiers (for example sphericity) and is best, if needed, to determine the porosity using a simple

DEM model by filling a container. The particle shape will also influence the changes in bulk density during material flow and either dilation or compaction can be observed. Examples include the flow out of shallow hoppers and bins where there is a change in density in the vicinity of the opening which governs the flow rate. The angle of dilatancy can be measured in a direct shear test.

2. The bulk friction (shear) behaviour is strongly influenced by the particle shape, for example the angle of repose or direct shear tests. The less spherical the shape is, the higher the interlocking effect and thus the higher the bulk friction. However, the bulk friction is also strongly influenced by the sliding and rolling coefficients of friction, which, in combination with spherical particles can also produce accurate levels of bulk friction.
3. The effect of particle shape on energy dissipation is negligible.
4. The effect of particle shape on bulk stiffness is negligible.
5. The discharge rate will be influenced.
6. As mentioned previously, spherical particles are computationally the most efficient. The higher the complexity of the particle shape (by mathematical description or number of sub-particles) the longer the calculation of a defined simulation takes to complete.

6.2 Particle Size Distribution

For a reduction in the total number of particles in a given model and hence a reduction in the calculation time, the real particle size distribution (psd) of the bulk material is idealised by so called “exact scaling” or “coarse graining” approaches which multiply the real psd with a certain scale-up factor. For coarser material it might be appropriate to “scalp” or “cut” the real psd and hence, to neglect the fractions with finer particles. An overview about the existing approaches to modify the psd is given in [Roe18]. The effects of particle shape on the individual bulk properties are described below:

1. The psd will influence the packing porosity and hence the bulk density for a given particle density. Usually, with a wider psd, the porosity decreases. The effect can be modelled by filling a container.
2. The bulk friction (shear) behaviour is weakly influenced by the psd.
3. The effect of psd on energy dissipation is negligible.
4. The effect of psd on bulk stiffness is negligible.
5. A reduction in the total number of particles in a given model results in a logarithmic reduction in the calculation time.

In some instances it is necessary to represent the entire simulation assembly as larger particles. Here, the psd becomes almost arbitrary as the entire distribution range of the modelled particles are larger than those handled in practice. These situations require secondary validation (continuum methods, additional calibration tests or bigger scale verification) to ensure the bulk volume is not over represented and are predominantly qualitative in nature.

To prevent simulated calibration test apparatus dimensions influencing the results of the simulations, the control volume geometry must be a minimum of 5-10 times larger than the maximum particle size simulated and in some situations up to 20 times larger may be required. Particle size modelled should be based on the that which will provide meaningful results when modelling the full scale application in an acceptable time frame, taking into

consideration any possibility of sensitivity analysis required (such as operating conditions for example). Particle size used in the simulation of the calibration tests should also match those that will be used in the full scale application. Where this is not possible (for example due to the size of the experimental calibration test apparatus volume) suitable scale-up procedure should be followed.

6.3 Particle Density

In order to accurately model the mass flow rate and volume flow rate, the bulk density should be accurately modelled, despite the idealised psd and particle shape. When spherical particles are used, the porosity can be easily calculated as $\rho = (V_{\text{bulk}} - V_{\text{particle}})/V_{\text{bulk}}$ where V_{bulk} is the total volume occupied by the material including the voids and V_{particle} is the total solid volume occupied by the particles. With the porosity also given by $\rho = 1 - \rho_{\text{bulk}} / \rho_{\text{particle}}$ and the measured bulk density ρ_{bulk} known (measured), the particle density ρ_{particle} can be easily calculated to ensure the bulk density is correctly modelled. This is relatively easy for spherical particles since the volume V_{particle} can be easily calculated. For non-spherical particles and especially multi-sphere particles comprised of overlapping spheres, the volume of the particles is not that easily calculated and the porosity unknown. In this case, the modelled bulk density should be determined by modelling a filled container. From this, the porosity can then be calculated and if needed, the particle density adjusted to ensure the correct bulk density is modelled.

The porosity is also dependent on the frictional parameters and must be re-calculated if frictional parameters are changed during the calibration process. The effects of particle density on the individual bulk properties are described below:

1. The particle density has a strong influence on the bulk density following a linear relation for a given porosity.
2. The effect of particle density on the bulk friction (shear) behaviour is negligible.
3. The effect of particle density on energy dissipation is negligible.
4. The effect of particle density on bulk stiffness is negligible.
5. The particle density highly influences time step: the higher the particle density the larger the time step.
6. The particle density influence in flowability.

6.4 Contact Stiffness

The contact stiffness in the normal and tangential directions is used to calculate the contact forces. The formulation of the contact stiffness depends on the specific contact model used and even on the specific DEM code or software used. It is important to distinguish between the “particle/wall stiffness” and the “contact stiffness” and the user should be aware of which value is used in the specific DEM model. If the particle or wall stiffness is specified, the contact stiffness is calculated at run time by combining the stiffness of the two entities in contact (particle-particle or particle-wall). However, in some models the contact stiffness is directly specified for each type of contact (particle-particle and particle wall) and material.

If a simple linear contact model is used, the contact or particle/wall stiffness in the normal and tangential directions is specified by the user with units of N/m. If the particle/wall

stiffness is specified, the contact stiffness is calculated at run time by assuming two elastic springs in series,

$$k_n = k_1 k_2 / (k_1 + k_2)$$

For hysteresis contact model, a loading stiffness is typically specified.

If the Hertz-Mindlin (no-slip) model is used, it is usual for the user to specify the particle and wall Young's modulus and Poisson's ratio. At run time, the contact stiffness k_n in the normal direction is calculated as

$$k_n = 4/3 E^* \sqrt{R^* \delta_n}$$

where the effective (or contact) Young's modulus and contact curvature are given by

$$1/E^* = (1 - \nu_1^2)/E_1 + (1 - \nu_2^2)/E_2 \quad \text{and} \quad 1/R^* = 1/R_1 + 1/R_2$$

with Poisson's ratio ν and the subscripts 1 and 2 for the two entities (particle or wall) in contact. The contact overlap in the normal direction is given by δ_n . Similarly in the tangential direction, the contact stiffness is given by

$$k_t = 8G^* \sqrt{R^* \delta_n}$$

where the effective shear modulus is given by

$$1/G^* = 2(2 - \nu_1)(1 + \nu_1)/E_1 + 2(2 - \nu_2)(1 + \nu_2)/E_2$$

In some DEM codes the user does not specify the elastic properties of the individual entities but rather the contact (or effective) properties, for example E^* and G^* are directly specified for each type of contact and material.

In the Hertz-Mindlin model the contact stiffness is not only dependent on the overlap, but also on the particle size, which is not the case in the linear model. Poisson's ratio is only used to calculate the effective contact Young's modulus as well as the shear modulus. As such, the effect of Poisson's ratio is negligible in terms of bulk material behaviour and a value of 0.3 is usually assumed.

The effects of the contact stiffness on the individual bulk properties are described below:

1. The contact stiffness has a negligible effect on the bulk density.
2. The contact stiffness has an effect on the bulk friction only for unrealistically low stiffness values [Coet09] which should be avoided.
3. The contact stiffness on energy dissipation is negligible.
4. The contact stiffness has a strong relation with the bulk stiffness (for example measures in a uniaxial compression test). With an increase in the contact stiffness, the bulk stiffness increases.

5. The contact stiffness highly influences the time step: the higher the stiffness, the smaller the time step. Due to the effect on the time step, many DEM simulations use a reduced stiffness.

With the Hertz-Mindlin contact model, realistic bulk flow results can often be achieved using relatively low values for Young's modulus, starting at $1e7$ Pa and calibration is not necessary and often not performed. For the linear contact model, a lower-end contact stiffness would be in the order of $1e4$ N/m. If forces or pressures have to be measured it must be determined, how the reduction of the Young Modulus is influencing the simulation result. How this can be done is described in detail in [Lom14].

6.5 Contact Sliding Friction: Particle-Particle

The particle-particle coefficient of friction can not be directly measured due to the shape and size of typical particles. For the simulations, the particle shape and size have to be idealised for computational efficiency and the combination of particle shape, size, sliding and rolling friction has to produce realistic bulk flow behaviour. In other words, the coefficient of friction (amongst other parameters) has to compensate for the idealisations made and the final value used for the coefficient of friction is not necessarily that between two physical particles of the same material.

The effects of particle-particle sliding friction on the individual bulk properties are described below:

1. The particle-particle sliding friction has a weak influence on the bulk density. Higher friction values lead to less dense packings (slightly higher porosity).
2. The particle-particle sliding friction is one of the major parameters influencing the bulk friction (shear) behaviour. An increase in the sliding friction increases the bulk friction in an asymptotic relation. For lower friction coefficients, an increase results in a large increase in bulk friction, while for higher friction coefficients, the increase in bulk friction becomes negligible.
3. The particle-particle sliding friction is one of the major mechanisms for energy dissipation in the numerical model.
4. The effect of particle-particle sliding friction on the bulk stiffness is negligible.
5. The effect of particle-particle sliding friction on the computation time is negligible.

6.6 Contact Sliding Friction: Particle-Wall

The particle-wall sliding coefficient of friction can be directly measured in wall shear tests or inclined wall tests. The value has to be measured for all wall materials where geometric surfaces have to be considered in the simulation model.

The effects of particle-wall sliding friction on the individual bulk properties are described below:

1. The particle-wall sliding friction has a negligible influence on the bulk density.
2. The particle-wall sliding friction is one of the major parameters influencing the bulk friction (shear) behaviour, especially shearing against a structure or wall, for example down a chute or into an excavator bucket.

3. The particle-wall sliding friction is one of the major mechanisms for energy dissipation in the numerical model.
4. The effect of particle-wall sliding friction on the bulk stiffness is negligible.
5. The effect of particle-wall sliding friction on the computation time is negligible.

6.7 Contact Rolling Friction

The rolling friction can not be directly measured. Sometimes different values are determined for the rolling friction between particle-particle contacts and between particle-wall contacts. However, due to the fact that the rolling friction considers/compensates primarily for the effect of the particles shape, it can also be assumed that only one rolling friction value is required for the calibration process. When spherical particles are used, rolling friction should be included, but when non-spherical particles are used the inclusion of rolling friction is not necessary.

The effects of rolling friction on the individual bulk properties are described below:

1. The rolling friction has a negligible influence on the bulk density.
2. The rolling friction, in combination with the sliding friction, has a strong influence on the bulk friction (shear) behaviour.
3. The rolling friction has a negligible influence on the dissipation of energy.
4. The effect of rolling friction on the bulk stiffness is negligible.
5. The effect of rolling friction on the computation time is negligible.

6.8 Contact damping / Coefficient of restitution:

The coefficient of restitution (CoR) can be measured via drop tests or needs to be determined in the calibration process. However, often the damping behaviour becomes a secondary influence if a stream of bulk material needs to be modeled. Many bulk materials show a relatively strong damping behaviour. Hence, a value between 0.2 and 0.4 is appropriate in most cases and selecting a value will reduce the number of parameters to be calibrated.

The effects of the coefficient of restitution on the individual bulk properties are described below:

1. The CoR has a negligible influence on the bulk density.
2. The CoR has a negligible influence on the bulk friction (shear) behaviour.
3. The CoR (together with sliding friction) is one of the major mechanisms for the dissipation of energy and the bulk damping characteristics.
4. The effect of CoR on the bulk stiffness is negligible.
5. The effect of CoR on the computation time is negligible.

7 Experimental Tests for Calibration

Experimental tests for calibration provide the link between properties reflective of physical behaviour and the DEM simulation parameters.

Real physical properties greatly assist the calibration process and selection of the necessary experimental test parameters. Physical properties include operating moisture content (or range), representative particle size distribution, compressibility (bulk density) and consolidation range relevant to the full scale application being modelled.

7.1 Requirements to the Calibration Test

Due to the nature of the calibration process, it is necessary to determine bulk material behaviour in an experimental test to use the test results for the calibration of DEM parameters. As discussed in the previous section, often it is necessary to calibrate at least the particle-particle sliding friction as well as the rolling friction value (necessary for spherical particles).

There are many possible calibration tests available. Some of the primary requirements to an “ideal” calibration test for the scope of this paper:

1. Should basically reflect the final application scenario of the DEM simulation. In our case the calibration test should consider or include
 - a low consolidation of the bulk material;
 - a rapid flow behaviour;
 - a free surface flow scenario.
2. Should be simple and quick to undertake experimentally and in simulation;
3. Should require only a small amount of bulk material;
4. Should give a test result which can be easily determined also in the simulation;
5. Should give size invariant results. This means that the procedure should give the same test results independent from the size of the test apparatus. The determination of an angle is typically invariant to particle and test size if the flow behaviour which leads to the establishment of the angle is not significantly influenced by test size.

While requirement 1 is mandatory, the other requirements are optional and a calibration test might work even if not all requirements 2-5 are fulfilled.

To avoid an influence of the scaled or scalped psd in the simulation, the calibration test should have the size to consider the simulated psd without additional interaction with boundary or geometric conditions. A typical example for this problem is mechanical arching or bridging of particles above small outlets. The outlet size in experimental test must have a size which is large enough to enable the flow of the scaled or scalped particles in the simulation.

7.2 Possible Calibration Tests

[Coe16] gives a comprehensive overview of possible calibration tests. All have their advantages and disadvantages.

7.2.1 Angle of Repose Test

To determine the Angle of Repose (AoR) several tests can be undertaken:

- Lifting cylinder test:
- Shear box, ledge or slump test
- Trap door test, hourglass test or cone test [Der16]
- Rotating drum test

All tests allow typically an optical measurement of the AoR, and do not necessarily lead to the same values due to the differences in kinetic energy between the tests. The determination of the AoR in the simulations should consider, that the AoR is measured in several sections where a constant AoR can be found. An measurement algorithm for the AoR determination using lifting cylinder simulations can be found in [Wen12].

As described in [Roe18] the lifting cylinder test delivers NOT size invariant results due to the influence of the cylinder speed and the resulting gap effect.

The shear box, or ledge test or slump test considers a simple box with a removable side wall. The AoR is established of the remaining material bed in the box after the material flow out caused by the removed side wall. The shear box test delivers size invariant AoR results due to the rapid flow out of the material. Further the remaining mass in the shear box can be determined and used as an additional calibration result.

The rotating drum test can be used to measure the dynamic angle of repose. It is recommended to perform this test in the so-called rolling regime which is defined by the Froude number in the range $10^{-4} < Fr < 10^{-2}$ where

$$Fr = \omega^2 R / g$$

with ω the rotation speed, R the drum radius and g the gravitational acceleration. It is further advised that the ratio of the drum diameter to the particle diameter should be 25 or more for reliable results [Coe19].

7.2.2 Discharge Test

The measurement of the discharge time or mass flow rate is the aim of the discharge test. Often the mass flow rate of a bin or hopper is measured. The discharge time or mass flow rate as well as the remaining mass in the system can be measured as an additional parameter with any calibration test. Visual observation of coloured horizontal particle layers or markers allows the analysis of the flow regime.

7.2.3 Draw Down Test

The so called Draw Down Test (DDT) is a combination of the AoR and discharge test and is described in detail in [Roe19]. Material flows through an outlet with adjustable width from a upper box to a lower box. With the DDT the AoR can be determined for a active and passive flow condition. Similar to the AoR resulting from the lifting cylinder test = active flow condition and the shear box test where the AoR is established by the remaining material = passive flow condition).

With the DDT two AoRs and the mass flow rate and the discharge mass (in the lower or upper container) can be measured. As described in section 9. the four test results within one test bring a lot of advantages for this test.

Walls of the box may restrict flow to an upper maximum particle size modelled. An alternative approach is to form a small unrestricted stockpile of material and release a portion of the floor underneath it.

7.2.4 Inclining Wall Friction Test

The wall friction test is used to determine the static and dynamic friction properties between the assembly of particles and the boundaries or surfaces in the model. The test may also be used to assess the influence of rolling friction. A variety of methods exists for this test, the simplest consisting of individual particles or a bed of particles sitting on top of a horizontal surface. The surface is inclined to the horizontal and the angle to the horizontal at which particle slide is measured giving the static friction. Once particles slide, their velocity can be tracked to approximate the dynamic coefficient of friction.

7.2.5 Direct Shear Test for Internal and Wall Friction

The direct shear test can be performed in a translational shear cell or a annular ring (rotating) shear cell. In the translational test the maximum strain is limited by the geometrical constraints while the strain is unlimited in the rotating cell. However, in both cases the commercially available equipment is designed for geotechnical applications and thus relatively small (up to 300 mm x 300 mm) and not ideal for materials where the particles are larger than approximately 20 mm. Larger shear cells are not readily available [Coe16]. The test does however allow for the measurement of bulk friction and (apparent) cohesion as well as dilatant behaviour.

The test can also be used to measure the particle-wall friction. The determination of the wall friction using shear test is different from an inclined wall test discussed in Section 8.2.6 as the influence of applied normal stress can be evaluated with a wall friction shear test. This interaction of a bulk solid with boundary or equipment materials is an important factor to consider when designing and modelling mass flow hoppers, chutes, feeders and other equipment where flow is expected to occur.

Proper calibration of the relationship between the normal wall stress and shear stress is required to obtain reliable DEM predictions for design and modelling application. Typically the relationship between the normal and shear stress on a wall material is measured using a Jenike direct shear tester or ring shear tester to evaluate a wall yield locus and the variation of wall friction angle with normal stress. The experimental results from a wall friction tester can be used to conduct similar experiments in DEM to examine the shear stress with the variation of normal stress to calibrate parameters such as particle shape, particle to wall static and rolling friction and particle stiffness. Grima and Wypych [Gri13] developed a large-scale wall friction tester with a 300mm shear cell to examine the sensitivity of mechanical properties (viz. particle shape and stiffness) and contact model parameters on the measured variation of wall friction angle with normal stress in DEM simulations.

7.2.6 Uniaxial Confined Compression Test

In this test a container is filled with bulk material and then closed with a lid and compressed. The maximum compression pressure should be of the same order as the maximum pressure expected to act on the material in the final application to be modelled. During the test the load-displacement curve is measured and the slope of the loading curve used to define a bulk stiffness. The experiment is repeated numerically and the results are sensitive to only the particle/contact stiffness which makes this an ideal experiment to reverse calibrate the stiffness. The container should be large enough to minimise the wall effects and it is suggested that the size of the container (usually cylindrical) should be at least equal to 10 particle diameters.

7.2.7 Drop and Pendulum Tests

Drop and pendulum tests are used to measure or estimate the coefficient of restitution (CoR). The drop test is performed by dropping a single particle onto a flat surface manufactured from the material of interest. Using optical methods, the velocity just before and after impact or the rebound height can be used to calculate the CoR. Although this works well for spherical particles, it is less successful for non-spherical particles where the three-dimensional path of rebound needs to be recorded including particle rotation. The method is also not suitable for particle-particle contact. Pendulum tests as described in [Hlo18] offer some advantages in this regard. Drop tests and pendulum tests are methods for determining particle properties rather than calibration tests, such as the compression test for the elasticity modulus.

7.2.9 Penetration Test

Specifically for excavation processes such as grabs, buckets a penetration test can be used to calibrate the material equipment interaction properties. This is done by measuring the penetration resistance of a relevant tool shape as a function of depth. The container should be large enough to avoid wall effects. Material preparation can include a compression phase if it is relevant for the application and if the material is sensitive to compression.

8 DEM Studies with Varying Parameters

As described earlier, the contact model parameters need to be determined via running a series of DEM simulation with varying parameters. The parameters can be varied systematically or via an optimisation algorithm.

The systematic variation is time consuming due to the high number of necessary simulations. But it also allow an understanding of the general dependency of the macroscopic simulation result to the varied parameters.

As described in [Wen12] the determination of the AoR using a lifting cylinder tests while varying the particle-particle sliding coefficient μ_p and the rolling friction coefficient μ_r results in the following diagram.

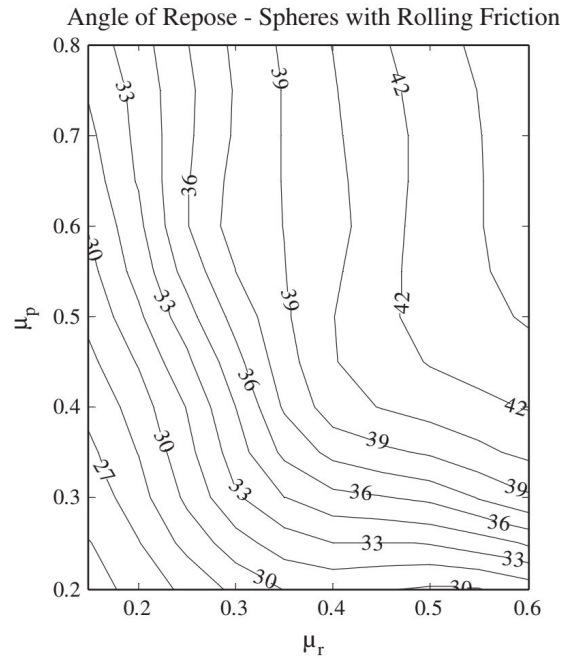


Fig. 2: AoR simulation results according to [Wen12] using a lifting cylinder test for a systematic variation of particle-particle sliding friction μ_p and rolling friction μ_r . The same macroscopic AoR is visualised with an isoline.

This result demonstrate clearly that there is a endless number of combination between μ_p and μ_r which result in the same macroscopic AoR value. This example highlights the problem of ambiguous parameter combinations. One calibration test result will not give a unique setting of two contact model parameters. The following section 10 gives advices how this problem can be solved.

An increasing number of calibration parameters increases this problem and brings classical visualisation techniques to its limits. Hence, if more than two parameters should be calibrated for example if one would include particle upscaling into calibration, the use of optimisation algorithms might be mandatory.

9 Identifying a Unique Set of DEM Parameters

The problem of ambiguous parameter combinations can be traced back to solving a mathematical equation with many unknown variables. If a number of unknown variables (=calibration parameters) should be determined, the same amount of independent equations are needed. Using this analogy, the calibration test should produce the same amount or more of “independent” test results.

This finding makes clear, why calibration tests which deliver more than one test results are preferable. The DDT as well as the direct shear test deliver four results. However, not all of the test results can be called independent. For instance, the two AoR results and the remaining mass in the upper or lower chamber of the DDT are depending on each other. The higher the AoR in the upper chamber, the higher the remaining mass here. In the direct shear test the shear response at different normal stresses can be used, as well as the internal friction angle and the time to reach failure.

With the task of superimposing different test results arise another problem. Not in all cases an intersection of the result isolines can be reached as described in [Der16]. Often the measurement error needs to be considered to enable a significant overlap of the test results as shown in detail in [Roe19]. Fig. 3 shows how the different test results with measurement error can be used for a tremendous decrease of possible parameter combinations. The use of optimisation algorithms together with multiple calibration objectives such as accuracy of different bulk parameters and particle upscaling to reduce computational times has been demonstrated in [Do19].

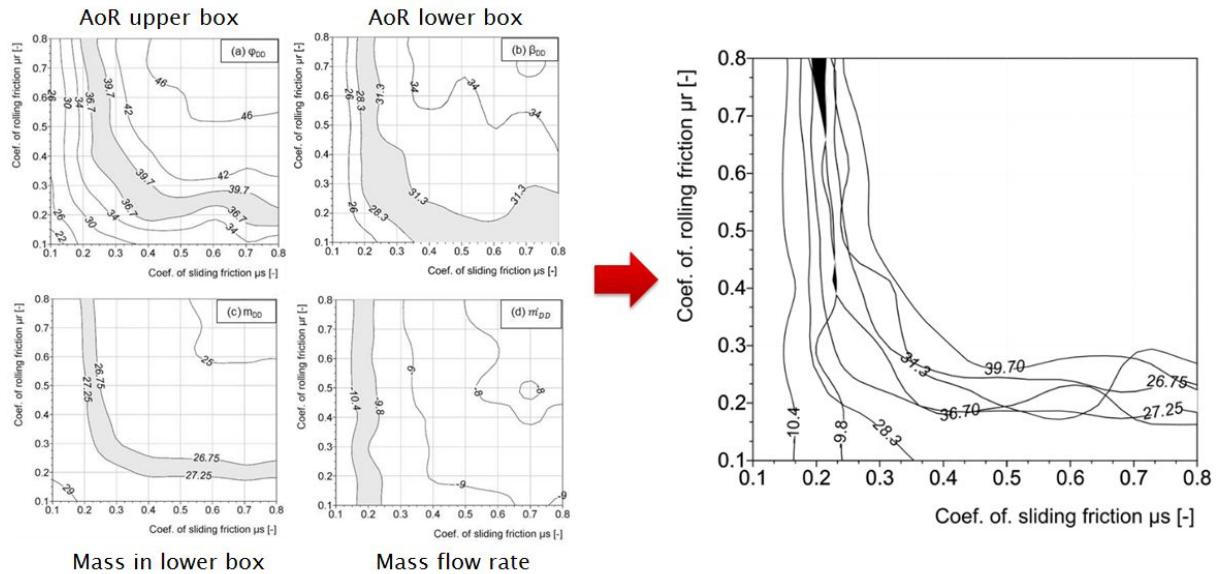


Fig. 3: Combination of DDT test results for gravel with consideration of the measurement error for the identification of a unique parameter setting.

The cumulation of the error between simulated and measured calibration result allows than a the definition of single parameter set.

If a basic understanding of the influence of the different calibration parameters to the calibration results is reached, an optimisation algorithm can be used for the faster determination of the calibration parameters.

10 Calibration Sequence

The ideal situation would be to have an experiment whose result is dependent on only a single unknown parameter. If such an experiment is available for each of the unknown parameters, calibration would be easier. Most of the experiments, when repeated numerically are, however sensitive to more than one parameter and therefore a number of experiments are needed to obtain a unique set of parameter values. However, if the calibration procedure of individual parameters is executed in a specific sequence, the need for iterations and finding the unique (optimal) set of parameters can be minimised.

The proposed sequence is given in the flowchart with reference to the sections where the influence of the specific parameter on the bulk behaviour is explained, as well as the proposed experiment(s) to calibrate the parameter value.

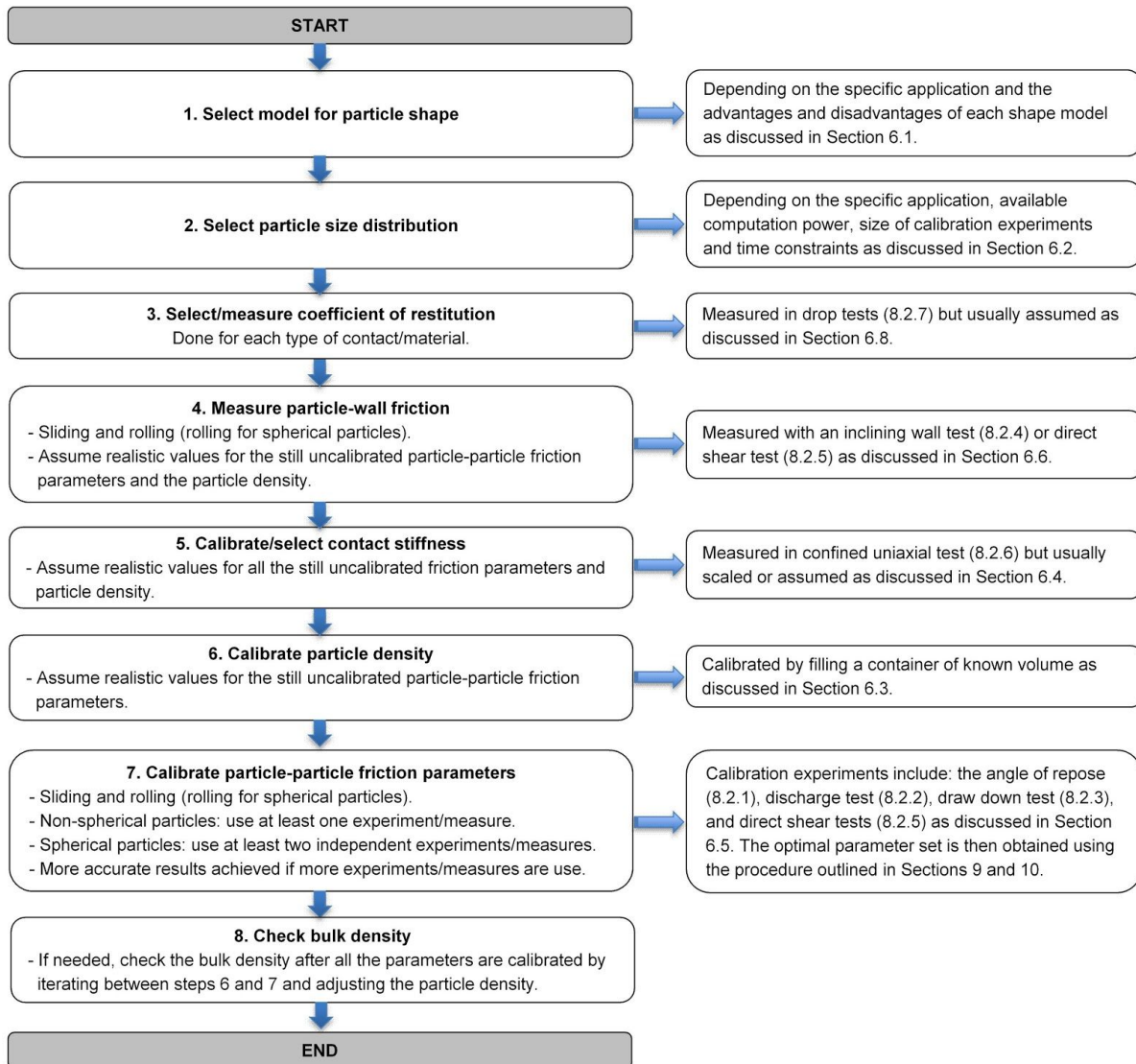


Fig: 4: Calibration sequence

References

- [Ai11] Ai, J., Chen, J.-F., Rotter, J.M., Ooi, J.Y.; Assessment of rolling resistance models in discrete element simulations, *Powder Technology* 206 (2011) 269–282.
- [Che17] Chen, W., Donohue, T., Katterfeld, A. Williams, K: Comparative discrete element modelling of a vibratory sieving process with spherical and rounded polyhedron particles. *Granular Matter* (2017) 19: 81.

- [Coe09] Coetzee, C.J.; Els, D.N.J.; Calibration of discrete element parameters and the modelling of silo discharge and bucket filling. *Computers and Electronics in Agriculture* 65 (2009) 198–212.
- [Coe16] Coetzee, C.J.: Calibration of the discrete element method and the effect of particle shape, *Powder Technology*, 2016 No. 297
- [Coe19] Coetzee, C.J.; Particle upscaling: Calibration and validation of the discrete element method. *Powder technology* 344 (2019) 487-503
- [Cun79] Cundall, P.A.; Strack, O. D. L.: A discrete numerical model for granular assemblies. *Geotechnique*, 29 (1979) 1, 47-65
- [Cun92] Cundall, P. A, Hart, R. D.: Numerical Modelling of Diskontinua. 1st US Conference on DEM, *Eng. Comput.*, 9 (1992) 2, 101-113
- [Der16] Derakhshani, S.M.; Schott, D.L., Lodewijks, G.: Micro macro properties of quartz sand: Experimental investigation and DEM simulation. *Powder Technology*, 269 (2015) 127-138
- [Do18] Do, H. Q.; Aragón, A. M.; Schott, D. L.: A calibration framework for discrete element model parameters using genetic algorithms. *Advanced Powder Technology* 29 (2018), 6, 1393-1403
- [Hlo18] Hlosta, J.; Zurovec, D.; Rozbroj, J.; Ramirez-Gomez, A.; Necas, J.; Zugzulka, J.: Experimental determination of particle-particle restitution coefficient via double pendulum method. *Chem.Eng.Des.* 2018, 135C, 222-233
- [Gri13] Grima, A.; Wypych, A.: Effect of Particle properties on the Discrete Element Simulation of Wall Friction, in 11th International Conference on Bulk Materials Storage, Handling and Transportation, (2013) Newcastle, Australia: University of Newcastle.
- [Grö16] Gröger, T.; Katterfeld, A.: On the Numerical Calibration of Discrete Element Models for the Simulation of Bulk Solids. *Computer Aided Chemical Engineering* 21. 2006
- [Li15] Li C., Xu, W.J., Meng, Q.S. (2015) Multi-sphere approximation of real particles for DEM simulation based on a modified greedy heuristic algorithm, *Powder Technology*, 286, (2015) 478-487.
- [Lom14] Lommen, S.; Schott, D.; Lodewijks, G.: DEM speedup: stiffness effects on behaviour of bulk material, *Particuology*, Vol. 12, 2014, pp. 107–112
- [Mar10] Markauskas, D.; Kacianauskas, R.; Džiugys, A.; Navakas, R.: Investigation of adequacy of multi-sphere approximation of elliptical particles for DEM simulations. *Granular Matter* 12 (1) (2010) 107–123.
- [Rad16] Radvilaitė, U.; Ramírez-Gómez, Á.; Kačianauskas, R.: Determining the shape of agricultural materials using spherical harmonics. *Computers and Electronics in Agriculture*. Vol. 128 (2016), 160-171.
- [Rah64] Rahman, A.: Correlations in the motion of atoms in liquid argon. *Phys. Rev.*, 136 (1964) 2A, 405-411
- [Rah11] Rahmann, M.; Schott, D. L.; Katterfeld, A.; Wensrich, C.: Influence of the software on the calibration parameters of DEM simulations. In: *Bulk solids handling. Section: Bulk Solids & Powder Science & Technology*. Vol. 31 (2011), 396-400

- [Roe18] Roessler, T.; Katterfeld, A.: Scaling of the angle of repose test and its influence on the calibration of DEM parameters using upscaled particles. Powder Technology. (330) 2018, 58-66.
- [Roe19] Rößler, T.; Richter, C.; Katterfeld, A.; Will, F.: Development of a standard calibration procedure for the DEM parameters of cohesionless bulk materials. Part I - Solving the problem of ambiguous parameter combinations. Powder Technology 343 (2019) 803–812
- [Wen12] Wensrich, C.; Katterfeld, A.: Rolling Friction as a Technique for Modelling Particle Shape in DEM. Powder Technology 217 (2012), 409–417